Journal of Translational Autoimmunity 7 (2023) 100203

Contents lists available at ScienceDirect

Journal of Translational Autoimmunity

journal homepage: www.sciencedirect.com/journal/journal-of-translational-autoimmunity

The effect of HLA-DRB1*04:01 on a mouse model of atherosclerosis

Garth Blackler [a], James Akingbasote [a], Ewa Cairns [a,b], Christopher Howlett [c,d], Patti Kiser [c], Lillian Barra [a,b,e,*]

[a] Department of Microbiology and Immunology, Western University, London, Ontario, Canada
[b] Department of Medicine, Division of Rheumatology, Western University, London, Ontario, Canada
[c] Department of Pathology and Laboratory Medicine, Western University, London, Ontario, Canada
[d] Department of Pathology and Laboratory Medicine, London Health Research Centre, London, Ontario, Canada
[e] Department of Epidemiology and Biostatistics, Western University, London, Ontario, Canada

ARTICLE INFO

Handling Editor: Dr Y Renaudineau

Keywords:
Rheumatoid arthritis
Atherosclerosis
Animal models
HLA-DRB1

ABSTRACT

Objectives: HLA-DRB1 is associated with an increased risk of cardiovascular disease in patients with rheumatoid arthritis (RA). This study aimed to determine the effect of HLA-DRB1 on atherosclerotic cardiovascular disease (ASCVD) using a novel mouse model.

Methods: Mice transgenic for HLA-DRB1*04:01 (DR4tg) were crossed with low density lipoprotein receptor knock-out (*Ldlr*$^{-/-}$) mice that develop atherosclerosis when fed a high fat, high cholesterol (HFHC) diet. Male and female DR4tg*Ldlr*$^{-/-}$ (n = 48), *Ldlr*$^{-/-}$ (n = 24), DR4tg (n = 24), and C57Bl/6 (B6) background (n = 24) mice were fed HFHC or regular diet (RD) for 12 weeks. Blood samples were analyzed for serum lipoproteins using a colorimetric assay. C-reactive protein (CRP) and oxidized LDL (OxLDL) were measured using ELISA. Atherosclerosis in the aortas was assessed using the lipid stain, Sudan IV. The presence of citrulline in atherosclerotic plaque was determined by immunohistochemistry.

Results: Sera low-density lipoprotein cholesterol (LDL-C) levels were higher in HFHC-fed *Ldlr*$^{-/-}$ versus DR4tg*Ldlr*$^{-/-}$-; p = 0.0056, but the aortic plaque burden and degree of citrullination in the plaque were similar for these two strains. The ratio of pro-atherogenic OxLDL to LDL levels was higher in DR4tg*Ldlr*$^{-/-}$ than *Ldlr*$^{-/-}$mice; p = 0.0017. All mice had an increase in CRP when fed a HFHC diet, most pronounced for DR4tg*Ldlr*$^{-/-}$; p = 0.0009. There were no significant sex differences for DR4tg*Ldlr*$^{-/-}$ mice; however, male *Ldlr*$^{-/-}$ mice had worse atherosclerosis. B6 and DR4tg mice did not have significant elevations in serum cholesterol levels and did not develop atherosclerosis.

Conclusions: Expression of HLA-DRB1 resulted in an elevation of OxLDL and a reduction in the male bias for atherosclerosis, mimicking what is observed in RA.

CRediT author statement

Lillian Barra: Conceptualization, Methodology, Validation, Resources, Writing – Original draft preparation, Visualization, Supervision, Project administration, Funding acquisition; **Ewa Cairns:** Conceptualization, Methodology, Validation, Resources, Writing – Original draft preparation, Visualization, Supervision, Project administration, Funding acquisition; **Garth Blackler:** Methodology, Validation, Formal analysis, Investigation, Resources, Data curation, Writing – Original draft preparation, Visualization, Project administration; **James Akingbasote:** Methodology, Validation, Formal analysis, Investigation, Resources, Data curation, Writing – Review and editing; **Christopher Howlett:** Methodology, Investigation, Writing – Original draft preparation; **Patti Kiser:** Methodology, Investigation, Writing – Original draft preparation.

1. Introduction

The HLA-DRB1 gene encodes the major histocompatibility complex II (MHCII) that binds and presents antigens to T cells. Several HLA-DRB1 alleles have been associated with various autoimmune and inflammatory conditions, including rheumatoid arthritis, polymyalgia rheumatica, giant cell arteritis, systemic lupus erythematosus, type I diabetes, and atherosclerotic cardiovascular disease (ASCVD) [1–5]. The role of HLA-DRB1 in the pathogenesis of immune dysfunction is best described

* Corresponding author. Western University, 268 Grosvenor St, Room D2, London, ON, N6A 4V2.
E-mail address: lillian.barra@sjhc.london.on.ca (L. Barra).

https://doi.org/10.1016/j.jtauto.2023.100203
Received 30 April 2023; Received in revised form 12 June 2023; Accepted 14 June 2023
Available online 21 June 2023

for rheumatoid arthritis (RA), a chronic inflammatory arthritis affecting approximately 0.5% of the global population with higher rates in North America [6].

In RA, HLA-DRB1 alleles encoding MHCII molecules with a consensus sequence in the antigen binding pocket known as the Shared Epitope confer the strongest genetic risk for RA across diverse ethnic and racial groups [7,8]. The Shared Epitope binds strongly to peptides containing the post-translationally modified amino acid, citrulline leading to the activation of T and B cells and subsequent production of anti-citrullinated protein antibodies (ACPA) [1,9,10]. ACPA are detected in >70% of RA patients, strongly associated with the Shared Epitope, highly specific for RA and predictive for erosive joint disease [1,11,12]. Although RA primarily affects synovial joints, ACPA may also directly cause injury to tissues in multiple organ systems, including the cardiorespiratory systems [13,14]. The risk of ASCVD in RA has been reported to be 50% higher than in the general population and this increased risk is more pronounced in RA patients expressing ACPA and/or the Shared Epitope [15,16]. The mechanisms by which ACPA and/or the Shared Epitope contribute to ASCVD in RA are unknown.

To better understand the role of HLA-DRB1 in the pathogenesis of atherosclerosis, we aimed to create and characterize a novel animal model. We bred HLA-DRB1*04:01 transgenic mice (DR4tg) [17] with a well-established model for atherosclerosis, low-density lipoprotein (LDL) receptor knock-out (*Ldlr*$^{-/-}$) mice [18,19]. Herein we describe the effect of HLA-DRB1*04:01 expression on lipid levels, systemic inflammation and atherosclerosis severity on the *Ldlr*$^{-/-}$ mouse model.

2. Materials and methods

2.1. Mice

B6.12S97-*Ldlr*^{tm1her}/J mice (referred to as *Ldlr*$^{-/-}$) on C57Bl/6 (B6) background (The Jackson Laboratory, Maine, USA) and HLA-DRB1*04:01 transgenic mice (DR4tg) on a B6 background [17] were bred in-house. B6 mice were purchased from The Jackson Laboratory (Maine, USA). DR4tg mice were crossed with *Ldlr*$^{-/-}$mice for 5 generations to establish a novel strain, DR4tg *Ldlr*$^{-/-}$. Genotyping was performed at Lawson Health Research Institute, London, Ontario to confirm the absence of the low-density lipoprotein receptor and the presence of the HLA-DRB1*04:01 insert (Supplementary Fig. 1). All experiments included male and female mice. Mice were housed and handled at the Animal Care and Veterinary Services barrier facility at Western University according to the guidelines of the Canadian Council on Animal Care. The study (protocol #2018-131) was approved by the Animal Care and Use Committee (Western University, London, ON, Canada).

After weaning, mice were fed a regular diet (RD) (Envigo, 8904: 4.7% fat, 40.2% carbohydrate, 24.3% protein) until they were 6–8 weeks old, then randomized to a high sucrose, high fat, high cholesterol diet (HFHC, Envigo: 21.2% fat, 48.7% carbohydrate, 17.3% protein, 0.2% cholesterol) or RD for 100 days and sacrificed. Mice were weighed at the beginning and end of the study. At sacrifice, blood was collected, and hind limbs, liver, heart, and aorta were harvested and fixed in 10% buffered formalin (Fisher Scientific, 245–685). Additionally, fat pads were dissected and weighed as a surrogate measure of centripetal obesity.

2.2. Serum lipid and C-reactive protein levels

Serum cholesterol, low-density lipoprotein cholesterol (LDL-C), and high-density lipoprotein (HDL-C) concentrations were determined using a colorimetric assay kit (Abcam, ab65390). Serum oxidized low density lipoprotein (OxLDL) was measured using ELISA (Lifeome Biolabs Inc, E07933m-96). Samples were tested in duplicate. C-reactive protein (CRP) serum concentrations were determined, in duplicate, using an ELISA kit (Abcam, ab157712).

2.3. Preparation of aorta

Periadventitial tissue was removed from the aortas. Aortic lipids were then stained with 5 mg/mL Sudan IV (Sigma, 198,102) for 40 min at 37 °C. Aortas were then washed in 70% isopropanol for 5 min at 37 °C, transferred to a dish containing 5% agarose and prepared *en face*. Aortic plaque burden was quantified as plaque area divided by total aortic area [20].

2.4. Histopathology

Formalin-fixed liver and aortic sinuses were sectioned at 5 μm thickness and stained with hematoxylin (Leica Biosystems, 3801562) and eosin (Fisher Scientific, E511) (HE). Liver sections were blindly assessed for non-alcoholic fatty liver disease using a modified scoring system based on Liang et al. [21]. In short, macrovesicular steatosis, microvesicular steatosis, hepatocyte hypertrophy and inflammatory cell foci were scored from 0 to 3 based on the area of involvement or number of inflammatory foci per microscopic field (100×, 3.1 mm^2), for a maximum total score of 12. Hepatic fibrosis was not assessed in this model. Citrullinated proteins were detected in the aortic sinus using an anti-modified citrulline (AMC) detection kit (Sigma Canada, 17–347B). Sections were permeabilized with a 0.25% triton-x solution in phosphate buffered saline (PBS) for 10 min at room temperature (RT). Antigen retrieval was performed using a trypsin retrieval kit (Abcam, ab970) at RT for 20 min. Endogenous peroxidases were quenched using a 3% solution of hydrogen peroxide and the samples were blocked with 10% goat serum (Thermo Fisher Scientific, PCN5000) in PBS for 30 min. AMC and a monoclonal human IgG1 lambda isotype control (Abcam, ab206203) were diluted in 1% goat serum to 0.0005 mg/mL and incubated at 4° overnight. Then, the sections were treated with the secondary antibody provided with the AMC kit (1/200 dilution in PBS and 1% goat serum) for 30 min at RT. Modified citrulline was visualized using ImmPact AMEC red substrate (Vector labs, SK-4285) and tissue was counterstained with Harris Hematoxylin (Leica Biosystems, 3801562). Slides were mounted using water-based mounting media (Vector, H-5501) and digitized on a Leica DM1000 (200× magnification). The surface area of tissue containing modified citrulline within the total plaque area was determined using ImageJ [22].

2.5. Statistical analyses

All statistical analyses were performed using GraphPad (version 9.2.0). Two-way ANOVA with multiple comparisons and Bonferonni's correction was used for analyses with >2 groups and Mann-Whitney to compare two groups. A p-value of ≤0.002 was considered significant.

3. Results

3.1. Weight distribution in mice fed a HFHC diet

All mice gained weight regardless of diet. However, B6 mice fed a HFHC diet compared to RD had significantly more weight gain (Fig. 1A): % increase in median weight [95% confidence interval (CI)] of 49.7 [40–70.1] vs. 23.3 [14.3–29]; $p < 0.0001$. Fat pad mass was significantly increased in *Ldlr*$^{-/-}$ on the HFHC diet vs. RD (Fig. 1B): 1.6 [1.1–1.9]% vs. 0.6 [0.5–1.1]%; $p = 0.0016$. Similarly, HFHC-fed DR4tg*Ldlr*$^{-/-}$ mice had a larger increase in fat pad mass than those fed RD: 1.4 [1.2–2.1]% vs. 0.3 [0.3–0.4]%; $p < 0.0001$ (Fig. 1B). Male and female mice had similar weight gain and fat pad mass (Fig. 1).

3.2. Effect of HLA-DR4 on circulating lipid levels, and CRP

As expected, the HFHC diet induced hypercholesterolemia in *Ldlr*$^{-/-}$ with a median value [95% CI] of 2460.0 [1812–2643] mg/dL compared to 289.6 [263.3–416.2] mg/dL in RD-fed mice of the same strain, p <

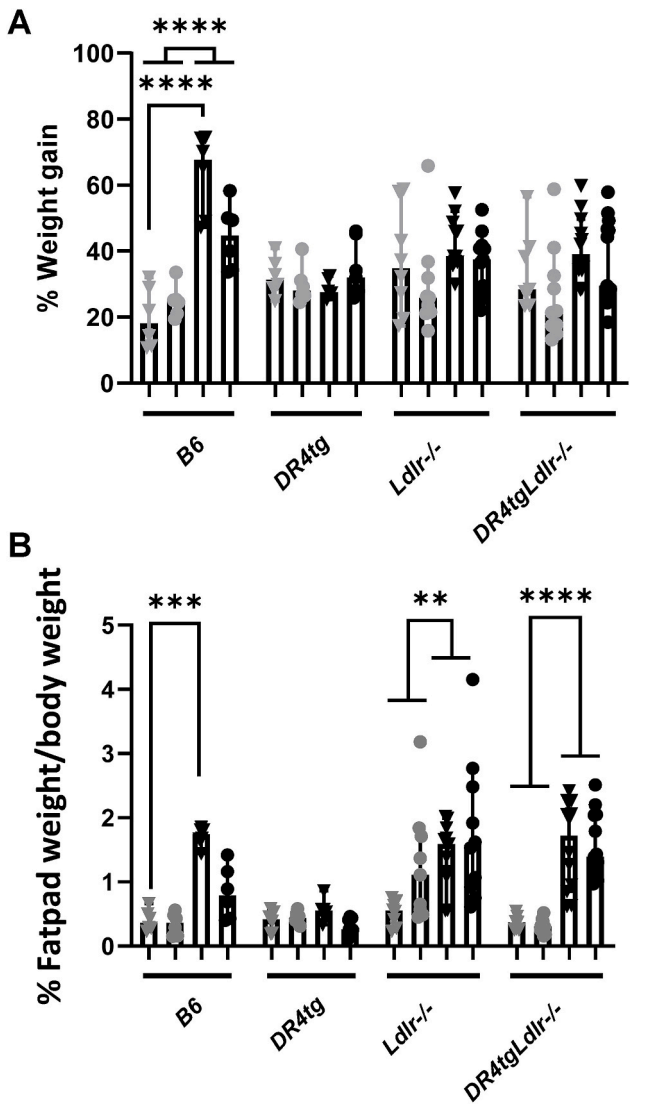

Fig. 1. DR4tg*Ldlr*$^{-/-}$ mice fed a HFHC diet had an increase in fat pad mass. Weight gain (A) and fat pad mass (B) of male (triangles) and female (circles) mice fed a RD (grey; n = 6–10) or HFHC diet (black; n = 6–13). Data are presented as median with 95% CI. Weight gain is reported as the % of weight gain at 100 days from baseline weight. Fat pad mass is reported as the % of total body weight at 100 days. **p < 0.002; ***p = 0.0007; ****p < 0.0001 by Two-way ANOVA with Bonferroni correction.

0.0001 (Fig. 2A). B6 and DR4tg mice did not develop hypercholesteremia when fed a HFHC diet. Total serum cholesterol levels in HFHC-fed DR4tg*Ldlr*$^{-/-}$ mice were elevated when compared to RD: 1265 [1046–1508] mg/dL and 249.4 [127.7–342] mg/dL, respectively; p < 0.0001. Serum LDL-C was significantly increased in HFHC-fed *Ldlr*$^{-/-}$ and DR4tg*Ldlr*$^{-/-}$ mice when compared to RD: 1502 [1286–1789] vs. 201.5 [154.3–276.1] mg/dL and 709.5 [654.7–1027] mg/dL vs. 127 [91.9–194.1] mg/dL, respectively; p < 0.0001 (Fig. 2C). However, serum total cholesterol and LDL-C was significantly lower in DR4tg*Ldlr*$^{-/-}$ compared to *Ldlr*$^{-/-}$ mice fed a HFHC diet, p < 0.0001 (Fig. 2AC). Additionally, HFHC-fed DR4tg*Ldlr*$^{-/-}$ mice had higher serum HDL-C than those fed RD: 412.4 [312.1–552.8] vs. 172.9 [124.6–233.7] mg/dL, respectively; and the other mouse strains regardless of diet (Fig. 2B); p < 0.001. The ratio of OxLDL to LDL-C was significantly higher in HFHC-fed DR4tg*Ldlr*$^{-/-}$ mice when compared to HFHC-fed *Ldlr*$^{-/-}$ mice: 53.31 [44.1–65.2] and 12.71 [0–31.6] nmol/dL, respectively (Fig. 2D); p = 0.0017. Female *Ldlr*$^{-/-}$mice were less likely than female DR4tg*Ldlr*$^{-/-}$ to have detectable OxLDL (2/6 vs. 6/6 mice). There were no other differences in serum lipids detected between sexes (Fig. 2E–H). CRP was elevated in all HFHC-fed animals, reaching significance in the DR4tg*Ldlr*$^{-/-}$ strain: 1.8 [1.3–2.4] μg/mL and 3.2 [2.7–4.1] μg/mL; RD vs HFHC respectively; p = 0.0009 (Fig. 3).

3.3. Liver histopathology in mice fed a HFHC diet

Mice fed a HFHC diet had the following histologic features that distinguished them from RD mice: macrovesicular steatosis, microvesicular steatosis, hepatocyte hypertrophy, and inflammatory infiltrate (Fig. 4A). Based on a histopathologic scoring system [21], all HFHC-fed mice had more severe non-alcoholic fatty liver disease (NAFLD) than RD-fed mice; p < 0.0001 (Fig. 4B). There was an uneven distribution of NAFLD phenotypes in HFHC-fed mice; inflammatory cell foci were mostly detected in *Ldlr*$^{-/-}$ and DR4tg*Ldlr*$^{-/-}$. Hepatocyte hypertrophy was infrequent in mice expressing HLA-DR4. Although all HFHC-fed mice manifested liver steatosis, DR4tg*Ldlr*$^{-/-}$ mice demonstrated a higher degree of macrovesicular steatosis than of microvesicular steatosis (Supplementary Fig. 2).

3.4. Atherosclerosis in mice fed a HFHC diet

Atherosclerotic plaque was only detected in *Ldlr*$^{-/-}$ and DR4tg*Ldlr*$^{-/-}$ mouse strains (Fig. 5). The aortic sinus walls of HFHC-fed *Ldlr*$^{-/-}$ and DR4tg*Ldlr*$^{-/-}$mice were markedly expanded by atherosclerotic plaques characterized by lipid-rich cores containing acicular cholesterol clefts mixed with variable amounts of mineralized material bordered by sheets of foamy macrophages and fibrous cap. Extracellular citrullinated proteins were identified within the lipid cores and intracellular citrullinated proteins within macrophages (Fig. 5A). The area within the plaque that contained citrullinated proteins was significantly higher in HFHC-fed *Ldlr*$^{-/-}$ mice (28.6 [5.2–53.7]%) and DR4tg*Ldlr*$^{-/-}$ mice (34.6 [15.1–48.8]%), compared to B6 (0 [0–1]%) and RD fed mice (0 [0–1]%); p < 0.0001. HFHC-fed *Ldlr*$^{-/-}$ and DR4tg*Ldlr*$^{-/-}$ mice had a similar degree of citrullination and there were no significant sex differences (Fig. 5B).

Aortic atherosclerotic plaque (Fig. 6A) was significantly higher in HFHC-fed *Ldlr*$^{-/-}$ and DR4tg*Ldlr*$^{-/-}$ mice compared to RD: 3.1 [2.3–5]% vs. 0.1 [0–0.1]%; p < 0.0001 and 3.1 [2.7–4.6]% vs. 0.2 [0.1–0.4]%; p < 0.0001, respectively (Fig. 6B). There were no significant differences detected between HFHC-fed *Ldlr*$^{-/-}$ and DR4tg*Ldlr*$^{-/-}$ mice. However, male *Ldlr*$^{-/-}$ mice had significantly more plaque than female *Ldlr*$^{-/-}$ mice (p = 0.0008). This sex difference was not seen in DR4tg*Ldlr*$^{-/-}$ mice (Fig. 6B).

4. Discussion

HLA-DRB1 Shared Epitope alleles are associated with increased cardiovascular risk in patients with rheumatoid arthritis; however, the mechanisms underlying this increased risk are poorly understood [16,23]. In this study, we used a novel mouse model (DR4tg*Ldlr*$^{-/-}$) and found that the expression of HLA-DRB1*04:01 resulted in altered serum levels of LDL-C and HDL-C, but a similar degree of atherosclerosis compared to HFHC-fed *Ldlr*$^{-/-}$ mice. Unlike *Ldlr*$^{-/-}$ where males developed more severe atherosclerosis, there were no detectable sex differences in DR4tg*Ldlr*$^{-/-}$

The *Ldlr*$^{-/-}$ mouse model is commonly employed to investigate the pathogenesis of atherosclerosis [24]. LDLR is ubiquitously expressed and is critical for the uptake and clearance of LDL-C from circulation. Although LDL-C has important roles in cellular homeostasis, including maintaining cell wall integrity, hormone synthesis and as a source of energy, excess circulating LDL-C (for example from diets rich in fat and cholesterol) leads to pathology in the liver and vascular tissues [25]. As expected, in our study, HFHC-fed *Ldlr*$^{-/-}$ mice developed elevated serum LDL-C, liver steatosis with inflammatory foci and atherosclerotic plaque when fed a HFHC diet.

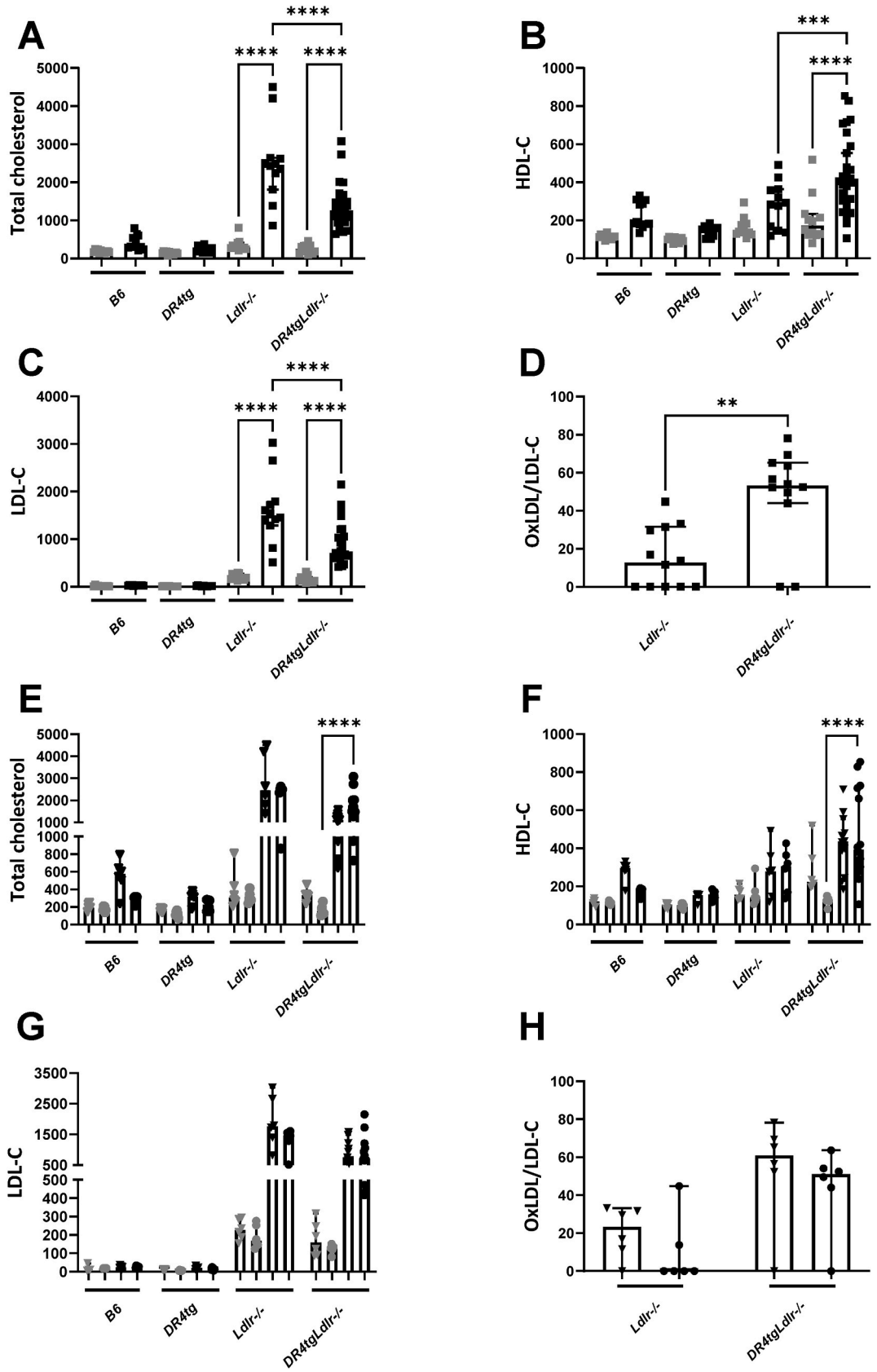

Fig. 2. Serum lipid levels are increased in DR4tg*Ldlr*$^{-/-}$ mice fed a HFHC diet. Total cholesterol (mg/dL) (A), HDL-C (mg/dL) (B), LDL-C (mg/dL) (C), and the ratio of OxLDL to LDL-C (nmol/dL) (D) at day 100 in mice fed RD (grey squares; n = 12) or HFHC diet (black squares; n = 12–25). Total cholesterol (mg/dL) (E), HDL-C (mg/dL) (F), LDL-C (mg/dL) (G), ratio of oxidized LDL to LDL-C (nmol/dL) (H) at day 100 in male (triangles) and female (circles) mice fed RD (grey; n = 6) or HFHC diet (black; n = 6–13). Data are presented as median with 95% CI. ***p = 0.0005; ****p < 0.0001 by Two-way ANOVA with Bonferroni correction, **p = 0.0017 by Mann-Whitney analysis.

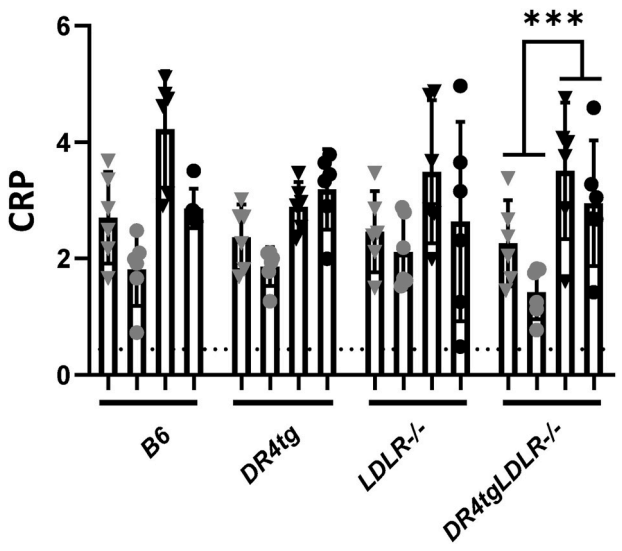

Fig. 3. CRP was elevated in DR4tg*Ldlr*$^{-/-}$ mice fed a HFHC diet. Sera at day 100 were tested for CRP (μg/mL) in mice fed a RD (grey; n = 12) or HFHC (black; n = 12) diet (male and female mice are represented by triangles and circles, respectively). Data are reported as median with 95% CI. ***p = 0.0009 by Two-way ANOVA with Bonferroni correction.

Similarly, HFHC-fed DR4tg*Ldlr*$^{-/-}$ developed non-alcoholic fatty liver disease and atherosclerotic plaque. Interestingly, the degree of hepatic and vascular disease was similar between *Ldlr*$^{-/-}$ and DR4tg*Ldlr*$^{-/-}$ despite the DR4tg*Ldlr*$^{-/-}$ mice having lower serum levels of LDL-C. This finding is reflective of what is observed in RA where there is an inverse relationship between total cholesterol and ASCVD risk, a phenomenon termed "the lipid paradox" [26]. A potential factor contributing to the "lipid paradox" is the elevation of other more pro-atherogenic lipoproteins, such as OxLDL [27]. Similar to RA, we found a higher proportion of serum OxLDL in DR4tg*Ldlr*$^{-/-}$ than in *Ldlr*$^{-/-}$ mice. Oxidation of lipids changes their properties, interfering with cell membrane function, inhibiting enzymes, and leading to molecular instability with bioactive end-products, such as malondialdehyde (MDA) [28]. Elevated serum OxLDL and its by-products are associated with worse atherosclerosis and cardiovascular events [29]. OxLDL is taken up more readily by macrophages in the endothelium via scavenger receptors than unmodified LDL-C. The resulting foam cells release pro-inflammatory mediators and proteases, which contribute to the instability of plaque leading to rupture, thrombosis, and ischemic events. Additionally, foam cells become necrotic, releasing reactive oxygen species (ROS) and promoting further oxidation of lipoproteins, resulting in a detrimental cycle [30]. In the liver, OxLDL is scavenged by Kupffer cells leading to steatosis and inflammatory foci that predispose to fibrosis [31].

The mechanism by which HLA-DRB1*04:01 contributes to increased OxLDL is unknown. One study reported higher CRP in subjects expressing HLA-DRB1, suggesting a potential role for HLA-DRB1 in driving systemic inflammation, which promotes reactive oxygen species (ROS) [5] and subsequently the production of OxLDL. In our study, we detected significant CRP elevations in HFHC-fed DR4tg*Ldlr*$^{-/-}$, supporting the hypothesis that increased systemic inflammation can lead to oxidation of LDL-C.

In patients with RA, it has been reported that the association between Shared Epitope alleles and ASCVD was compounded by smoking and the expression of ACPA [16]. Smoking is frequent in RA patients and leads to ROS, oxidation and citrullination [28]. ACPA targets proteins containing citrulline, arginine post-translationally modified by peptidyl deiminase (PAD). This enzyme becomes active in the presence of calcium, which is tightly regulated within the cellular environment [32]. Calcium is also a major component of the atherosclerotic plaque. It can be released intra-cellularly under certain conditions present both in RA and atherosclerosis, including immune cell activation and apoptosis [32,33]. A recent study has proposed a direct role of MHCII containing the Shared Epitope in promoting citrullination by its interaction with calreticulin,

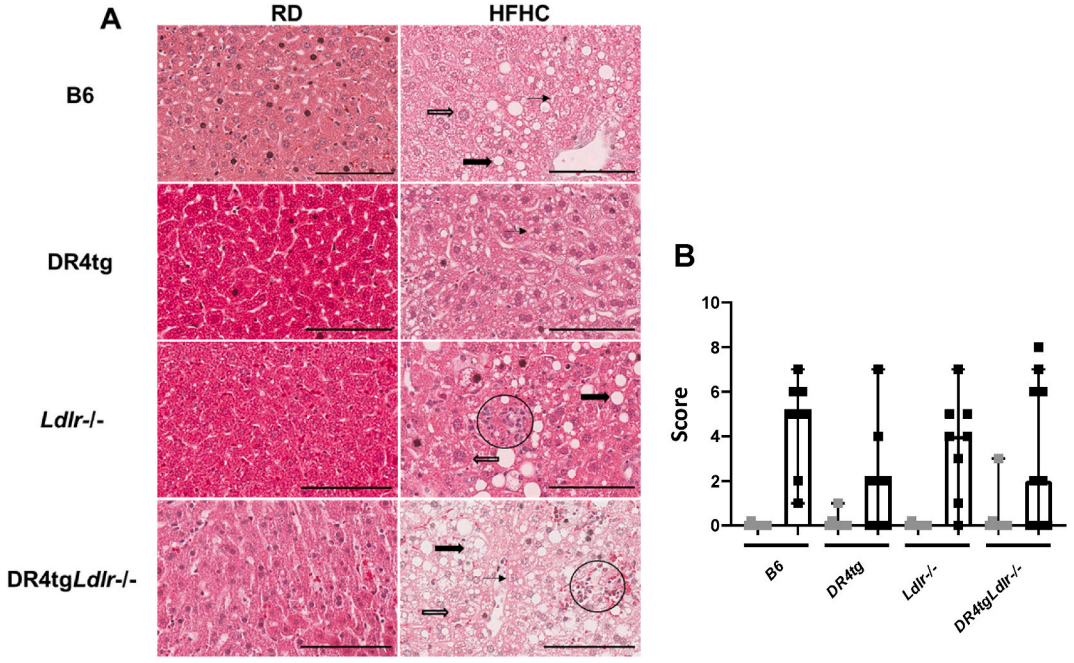

Fig. 4. Mice fed a HFHC have evidence of NAFLD. Representative histological images of the livers from B6, DR4tg, *Ldlr*$^{-/-}$, and DR4tg*Ldlr*$^{-/-}$ mice fed a RD versus HFHC diet (A). The following features of NAFLD were identified: macrovesicular steatosis (filled arrow), microvesicular steatosis (thin arrow), hepatocyte hypertrophy (hollow arrow), and inflammatory foci (circle). The NAFLD score of mice fed a RD (grey squares; n = 8–9) or HFHC (black squares; n = 8–9) diet at 100 days (B). Data are presented as median with 95% CI. RD vs. HFHC p < 0.0001 by Two-way ANOVA with Bonferroni correction. Scale bar represents 100 μm at a magnification of 400×.

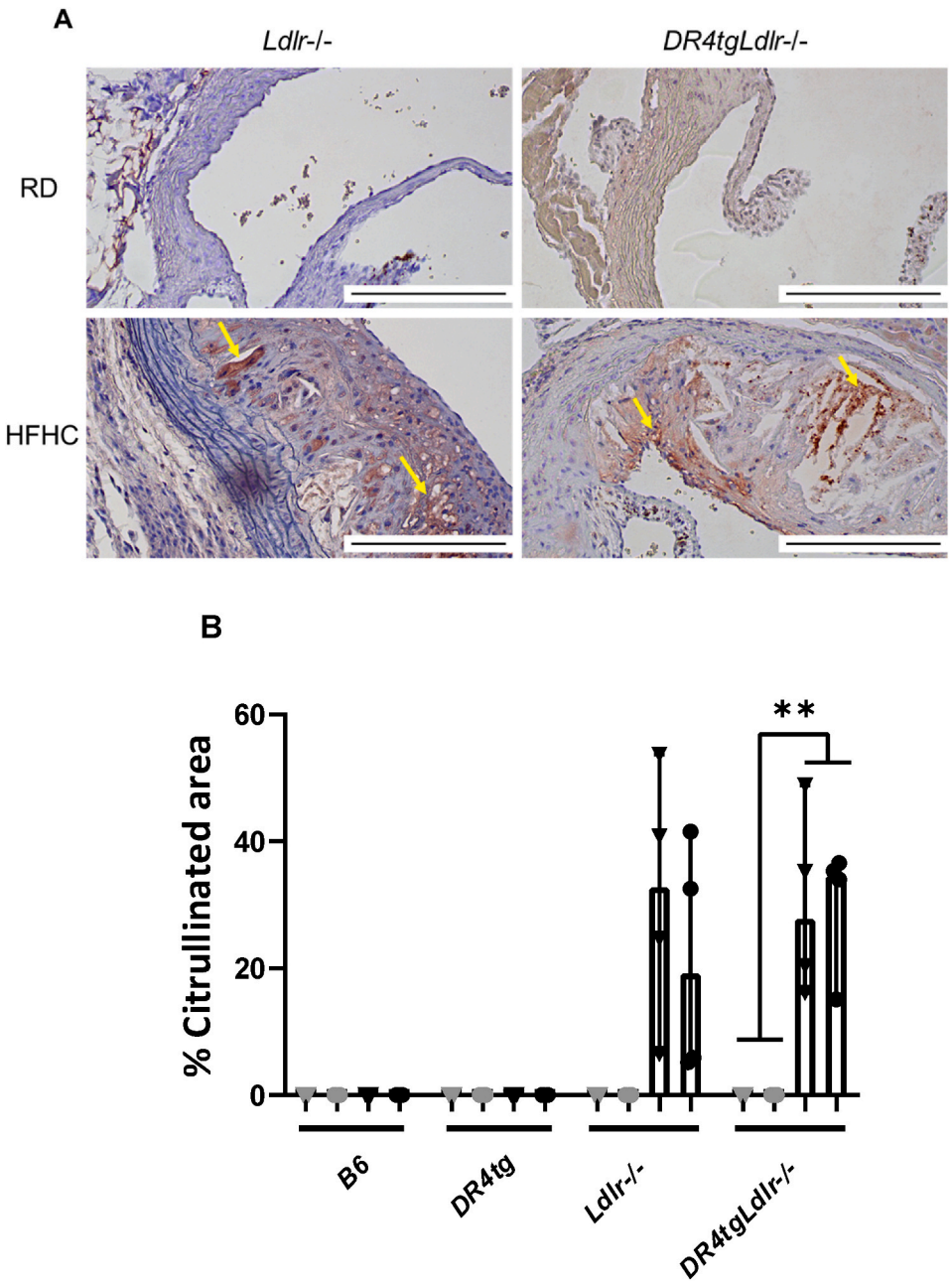

Fig. 5. Citrullinated proteins are present in atherosclerotic plaque. Representative histologic sections of aortic sinuses at day 100 stained for citrullinated proteins (brown), as denoted by yellow arrows, and counterstained with hemotoxylin (A). Extracellular citrullinated proteins are identified within the lipid cores and intracellular citrullinated proteins within macrophages. Quantification of citrullinated proteins is presented as the % surface area stained in brown to total plaque area (B). Citrullinated proteins in the plaque of male mice (triangles) and female mice (circles) fed a RD (grey; n = 2–4) or HFHC diet (black; n = 2–4) (B). Data are reported as median with 95% CI. **p = 0.0012 by Two-way ANOVA with Bonferroni correction. Scale bar represents 200 μm at a magnification of 200×.

an innate immune receptor that can initiate a signal transduction cascade leading to calcium mobilization. This signaling cascade can also lead to the production of nitrogen oxide with the potential for lipid oxidation [34].

We detected citrullinated proteins extra-cellularly and within macrophages, including lipid-laden macrophages (foam cells) in the atherosclerotic plaque of HFHC-fed *Ldlr*$^{-/-}$ and DR4tg*Ldlr*$^{-/-}$ mice. This is consistent with prior studies of *Ldlr*$^{-/-}$ mice [35] and ASCVD patients [14]. The extent of the citrullination did not appear to differ significantly between *Ldlr*$^{-/-}$ and DR4tg*Ldlr*$^{-/-}$ mice; however, the study was limited in that a semi-quantitative method was used. In addition, the AMC antibody we used for detecting citrulline cannot distinguish it from homocitrulline [36]. Thus, it is possible that the modified proteins detected in the plaque with AMC contain homocitrulline, citrulline or both. Two previous studies using mass spectrometry confirmed the presence of citrullinated and homocitrullinated proteins separately within atherosclerotic plaque of patients with ASCVD [14,37]. The presence of these modified proteins may be reactionary to the inflammatory atherosclerotic processes. However, homocitrullinated and citrullinated LDL-C were shown to promote foam cell formation *in vitro* [37,38] and higher total serum homocitrullinated proteins were detected in patients with ASCVD compared to healthy controls [37], suggesting that these post-translationally modified proteins/lipoproteins may also directly contribute to atherosclerosis progression.

Atherosclerotic cardiovascular disease in the general population is more common in males. In our study and other prior studies, atherosclerotic plaque was more prominent in HFHC-fed male versus female *Ldlr*$^{-/-}$ mice despite similar LDL-C levels [39]. Interestingly, there was no difference in OxLDL levels for female and male DR4tg*Ldlr*$^{-/-}$mice, whereas most female *Ldlr*$^{-/-}$ mice had undetectable OxLDL. Serum levels of OxLDL may partially explain the less severe atherosclerotic disease detected in female *Ldlr*$^{-/-}$ but not female DR4tg*Ldlr*$^{-/-}$ mice [40]. Thus, the DR4tg*Ldlr*$^{-/-}$ mice appear to mimic what is seen in human RA, where the effect of male sex on ASCVD risk is less

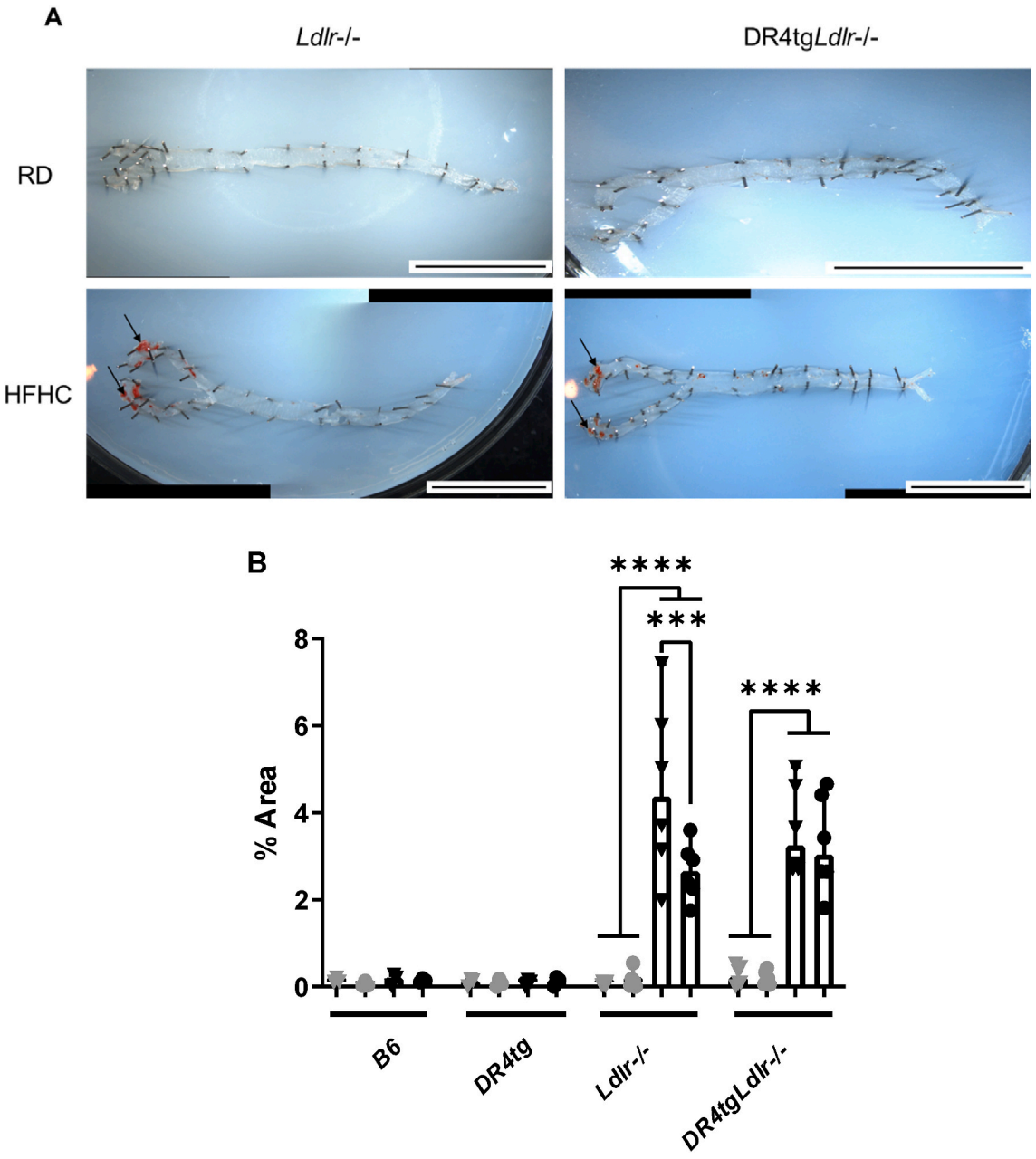

Fig. 6. Atherosclerotic plaque is present in the aortas of DR4tg*Ldlr*$^{-/-}$ mice fed a HFHC diet. Representative photographs of dissected aortas prepared *en face* and stained with Sudan IV from mice fed a RD or HFHC diet at day 100 (A). Arrows show lipid deposition stained in red within the aortic plaque. Quantification of aortic atherosclerotic plaque is presented as the % surface area stained in red to total aortic area. Aortic plaque area in male mice (triangles) and female mice (circles) fed a RD (grey; n = 3–6) or HFHC diet (black; n = 3–6) (B). Data are reported as median with 95% CI. ***p = 0.0008; ****p < 0.0001 by Two-way ANOVA with Bonferroni correction. Scale bar represents 1 mm at 2× magnification.

pronounced than what is seen in the general population [41]. Longer duration of HFHC diet may further accentuate these differences.

This study had some additional limitations. Lipoproteins other than those measured in this study could have contributed to the observed phenotype. For example, HDL-C was elevated in DR4tg*Ldlr*$^{-/-}$, but we did not measure subtypes of HDL-C, including "inflammatory HDL" that has been reported in RA and are associated with atherosclerosis [42]. Although this study suggests that HLA-DR4tg affects oxidation of lipids, particularly in female mice, the mechanism for this effect requires further study.

5. Conclusions

We have developed a mouse model that recapitulates risk factors for RA and cardiovascular disease, including the HLA-DRB1 gene, centripetal obesity, and dyslipidemia. When fed a high fat, high cholesterol diet, these mice developed atherosclerosis with the loss of male bias, similar to what is seen in RA. Future work using this model can elucidate mechanisms by which HLA-DRB1 interacts with sex and the environment to contribute to ASCVD risk in RA and other inflammatory conditions.

Funding sources

The study was funded by The Arthritis Society (Grant# YIO-14-123) and the Program of Experimental Medicine, Department of Medicine, Western University. E.C. was supported by the Calder Foundation and J. A. by the Bone and Joint Institute, Western University. No funding source was involved in the study design, data collection, analysis, interpretation, writing, or journal selection.

Availability of data and materials

The datasets supporting the conclusions of this article are included within the article and its additional files.

Declaration of competing interest

The authors declare that they have no known competing financial interests or personal relationships that could have appeared to influence the work reported in this paper.

Data availability

Data has been provided in the supplementary material

Acknowledgements

We would like to thank the laboratory of Dr. Murray Huff for their assistance with training for the preparation of aortic sinus sections.

Abbreviations

ACPA	Anti-Citrullinated Protein/Peptide Antibodies
AMC	Anti-Modified Citrulline
ASCVD	Atherosclerotic Cardiovascular Disease
B6	C57Bl/6
CRP	C-Reactive Protein
DR4tg	Human Leukocyte Antigen-DRB1*04:01 transgenic
DR4tg*Ldlr*$^{-/-}$	Low Density Lipoprotein Receptor knock-out mice transgenic for Human Leukocyte Antigen-DRB1*04:01
HDL-C	High Density Lipoprotein Cholesterol
HFHC	High Fat High Cholesterol Diet
HLA	Human Leukocyte Antigen
LDL-C	Low Density Lipoprotein Cholesterol
LDLR	Low Density Lipoprotein Receptor
Ldlr$^{-/-}$	Low Density Lipoprotein Receptor knock-out
MDA	Malondialdehyde
MHCII	Major Histocompatibility Complex II
OxLDL	Oxidized Low Density Lipoprotein
RD	Regular Diet
RA	Rheumatoid Arthritis
ROS	Reactive Oxygen Species
RT	Room Temperature

Appendix A. Supplementary data

Supplementary data to this article can be found online at https://doi.org/10.1016/j.jtauto.2023.100203.

References

[1] M. Bax, J. van Heemst, T.W. Huizinga, R.E. Toes, Genetics of rheumatoid arthritis: what have we learned? Immunogenetics 63 (8) (2011 Aug) 459–466, https://doi.org/10.1007/s00251-011-0528-6.

[2] C.M. Weyand, N.N. Hunder, K.C. Hicok, G.G. Hunder, J.J. Goronzy, HLA-DRB1 alleles in polymyalgia rheumatica, giant cell arteritis, and rheumatoid arthritis, Arthritis Rheum. 37 (4) (1994) 514–520, https://doi.org/10.1002/art.1780370411.

[3] L. Ortíz-Fernández, J. Martín, M.E. Alarcón-Riquelme, A Summary on the genetics of systemic lupus erythematosus, rheumatoid arthritis, systemic sclerosis, and sjögren's Syndrome, Clin. Rev. Allergy Immunol. (2022 Jun 24), https://doi.org/10.1007/s12016-022-08951-z (Epub ahead of print).

[4] J.A. Noble, A.M. Valdes, Genetics of the HLA region in the prediction of type 1 diabetes, Curr. Diabetes Rep. 11 (6) (2011) 533–542, https://doi.org/10.1007/s11892-011-0223-x.

[5] R. Paakkanen, M.L. Lokki, M. Seppänen, I. Tierala, M.S. Nieminen, J. Sinisalo, Proinflammatory HLA-DRB1*01-haplotype predisposes to ST-elevation myocardial infarction, Atherosclerosis 221 (2) (2012) 461–466, https://doi.org/10.1016/j.atherosclerosis.2012.01.024.

[6] K. Almutairi, J. Nossent, D. Preen, H. Keen, C. Inderjeeth, The global prevalence of rheumatoid arthritis: a meta-analysis based on a systematic review, Rheumatol. Int. 41 (5) (2021) 863–877, https://doi.org/10.1007/s00296-020-04731-0.

[7] P.K. Gregersen, J. Silver, R.J. Winchester, The shared epitope hypothesis. An approach to understanding the molecular genetics of susceptibility to rheumatoid arthritis, Arthritis Rheum. 30 (11) (1987 Nov) 1205–1213, https://doi.org/10.1002/art.1780301102.

[8] L.E. Dedmon, The genetics of rheumatoid arthritis, Rheumatology 59 (10) (2020) 2661–2670, https://doi.org/10.1093/rheumatology/keaa232.

[9] J.A. Hill, S. Southwood, A. Sette, A.M. Jevnikar, D.A. Bell, E. Cairns, Cutting edge: the conversion of arginine to citrulline allows for a high-affinity peptide interaction with the rheumatoid arthritis-associated HLA-DRB1*0401 MHC class II molecule, J. Immunol. 171 (2) (2003) 538–541, https://doi.org/10.4049/jimmunol.171.2.538.

[10] J. Kaur, E. Cairns, L. Barra, Restoring balance: immune tolerance in rheumatoid arthritis, J. Rheumatol. (2023), 220881, https://doi.org/10.3899/jrheum.220881 (Epub ahead of print).

[11] M.A.M. van Delft, T.W.J. Huizinga, An overview of autoantibodies in rheumatoid arthritis, J. Autoimmun. 110 (2020), 102392, https://doi.org/10.1016/j.jaut.2019.102392.

[12] M. van den Broek, L. Dirven, N.B. Klarenbeek, T.H. Molenaar, K.H. Han, P. J. Kerstens, T.W. Huizinga, et al., The association of treatment response and joint damage with ACPA-status in recent-onset RA: a subanalysis of the 8-year follow-up of the BeSt study, Ann. Rheum. Dis. 71 (2) (2012) 245–248, https://doi.org/10.1136/annrheumdis-2011-200379.

[13] A.J. Ytterberg, V. Joshua, G. Reynisdottir, N.K. Tarasova, D. Rutishauser, E. Ossipova, et al., Shared immunological targets in the lungs and joints of patients with rheumatoid arthritis: identification and validation, Ann. Rheum. Dis. 74 (9) (2015) 1772–1777, https://doi.org/10.1136/annrheumdis-2013-204912.

[14] J. Sokolove, M.J. Brennan, O. Sharpe, L.J. Lahey, A.H. Kao, E. Krishnan, D. Edmundowicz, C.M. Lepus, M.C. Wasko, W.H. Robinson, Brief report: citrullination within the atherosclerotic plaque: a potential target for the anti-citrullinated protein antibody response in rheumatoid arthritis, Arthritis Rheum. 65 (7) (2013) 1719–1724, https://doi.org/10.1002/art.37961.

[15] J.A. Avina-Zubieta, J. Thomas, M. Sadatsafavi, A.J. Lehman, D. Lacaille, Risk of incident cardiovascular events in patients with rheumatoid arthritis: a meta-analysis of observational studies, Ann. Rheum. Dis. 71 (9) (2012) 1524–1529, https://doi.org/10.1136/annrheumdis-2011-200726.

[16] T.M. Farragher, N.J. Goodson, H. Naseem, A.J. Silman, W. Thomson, D. Symmons, A. Barton, Association of the HLA-DRB1 gene with premature death, particularly from cardiovascular disease, in patients with rheumatoid arthritis and inflammatory polyarthritis, Arthritis Rheum. 58 (2) (2008) 359–369, https://doi.org/10.1002/art.23149.

[17] J.A. Hill, D.A. Bell, W. Brintnell, D. Yue, B. Wehrli, A.M. Jevnikar, D.M. Lee, W. Hueber, W.H. Robinson, E. Cairns, Arthritis induced by posttranslationally modified (citrullinated) fibrinogen in DR4-IE transgenic mice, J. Exp. Med. 205 (4) (2008) 967–979, https://doi.org/10.1084/jem.20072051.

[18] S. Ishibashi, M.S. Brown, J.L. Goldstein, R.D. Gerard, R.E. Hammer, J. Herz, Hypercholesterolemia in low density lipoprotein receptor knockout mice and its reversal by adenovirus-mediated gene delivery, J. Clin. Invest. 92 (2) (1993) 883–893, https://doi.org/10.1172/JCI116663.

[19] Y. Ma, W. Wang, J. Zhang, Y. Lu, W. Wu, H. Yan, Y. Wang, Hyperlipidemia and atherosclerotic lesion development in Ldlr-deficient mice on a long-term high-fat diet, PLoS One 7 (4) (2012), e35835, https://doi.org/10.1371/journal.pone.0035835.

[20] A.M. Archer, R. Saber, S. Rose, A. Shaffer, A.V. Misharin, F. Tsai, et al., ApoE deficiency exacerbates the development and sustainment of a semi-chronic K/BxN serum transfer-induced arthritis model, J. Transl. Med. 10 (1) (2016) 170, https://doi.org/10.1186/s12967-016-0912-y, 14.

[21] W. Liang, A.L. Menke, A. Driessen, G.H. Koek, J.H. Lindeman, R. Stoop, et al., Establishment of a general NAFLD scoring system for rodent models and comparison to human liver pathology, PLoS One 9 (12) (2014), e115922, https://doi.org/10.1371/journal.pone.0115922.

[22] M.D. Abramoff, P.J. Magalhaes, S.J. Ram, Image processing with ImageJ, Biophotonics 11 (2004) 36–42.

[23] L. Rodríguez-Rodríguez, R. López-Mejías, M. García-Bermúdez, C. González-Juanatey, M.A. González-Gay, J. Martín, Genetic markers of cardiovascular disease in rheumatoid arthritis, Mediat. Inflamm. 2012 (2012), 574817, https://doi.org/10.1155/2012/574817.

[24] S.C. Whitman, A practical approach to using mice in atherosclerosis research, Clin. Biochem. Rev. 25 (1) (2004) 81–93.

[25] G.W. Go, A. Mani, Low-density lipoprotein receptor (LDLR) family orchestrates cholesterol homeostasis, Yale J. Biol. Med. 85 (2012) 19–28.

[26] E. Myasoedova, C.S. Crowson, H.M. Kremers, V.L. Roger, P.D. Fitz-Gibbon, T. M. Therneau, S.E. Gabriel, Lipid paradox in rheumatoid arthritis: the impact of

serum lipid measures and systemic inflammation on the risk of cardiovascular disease, Ann. Rheum. Dis. 70 (3) (2011) 482–487, https://doi.org/10.1136/ard.2010.135871.

[27] A.M. Fernández-Ortiz, A.M. Ortiz, S. Pérez, E. Toledano, L. Abásolo, M. A. González-Gay, et al., Effects of disease activity on lipoprotein levels in patients with early arthritis: can oxidized LDL cholesterol explain the lipid paradox theory? Arthritis Res. Ther. 22 (1) (2020) 213, https://doi.org/10.1186/s13075-020-02307-8.

[28] H.B. Ferreira, T. Melo, A. Paiva, M.D.R. Domingues, Insights in the role of lipids, oxidative stress and inflammation in rheumatoid arthritis unveiled by new trends in lipidomic investigations, Antioxidants 10 (1) (2021) 45, https://doi.org/10.3390/antiox10010045.

[29] C. Meisinger, J. Baumert, N. Khuseyinova, H. Loewel, W. Koenig, Plasma oxidized low-density lipoprotein, a strong predictor for acute coronary heart disease events in apparently healthy, middle-aged men from the general population, Circulation 112 (5) (2005) 651–657, https://doi.org/10.1161/CIRCULATIONAHA.104.529297.

[30] K.J. Moore, F.J. Sheedy, E.A. Fisher, Macrophages in atherosclerosis: a dynamic balance, Nat. Rev. Immunol. 13 (10) (2013) 709–721, https://doi.org/10.1038/nri3520.

[31] V. Bieghs, F. Verheyen, P.J. van Gorp, T. Hendrikx, K. Wouters, D. Lütjohann, et al., Internalization of modified lipids by CD36 and SR-A leads to hepatic inflammation and lysosomal cholesterol storage in Kupffer cells, PLoS One 7 (3) (2012), e34378, https://doi.org/10.1371/journal.pone.0034378.

[32] V. Malmström, A.I. Catrina, L. Klareskog, The immunopathogenesis of seropositive rheumatoid arthritis: from triggering to targeting, Nat. Rev. Immunol. 17 (1) (2017) 60–75, https://doi.org/10.1038/nri.2016.124.

[33] D.G.F. Al-U'datt, B.G. Allen, R. Hiram, N. Alrabadi, Current knowledge into the role of the peptidylarginine deiminase (PAD) enzyme family in cardiovascular disease, Eur. J. Pharmacol. 891 (2021), 173765, https://doi.org/10.1016/j.ejphar.2020.173765.

[34] V. van Drongelen, W.H. Ali, J. Holoshitz, Uncovering a shared epitope-activated protein citrullination pathway, J. Immunol. 205 (3) (2020) 579–586, https://doi.org/10.4049/jimmunol.1901108.

[35] C. Yin, A.M. Vrieze, M. Rosoga, J. Akingbasote, E.N. Pawlak, R.A. Jacob, et al., Efferocytic defects in early atherosclerosis are driven by GATA2 overexpression in macrophages, Front. Immunol. 11 (2020), 594136, https://doi.org/10.3389/fimmu.2020.594136.

[36] J. Shi, A. Willemze, G.M. Janssen, P.A. van Veelen, J.W. Drijfhout, Cerami, et al., Recognition of citrullinated and carbamylated proteins by human antibodies: specificity, cross-reactivity and the 'AMC-Senshu' method, Ann. Rheum. Dis. 72 (1) (2013) 148–150, https://doi.org/10.1136/annrheumdis-2012-201559.

[37] Z. Wang, S.J. Nicholls, E.R. Rodriguez, O. Kummu, S. Hörkkö, J. Barnard, et al., Protein carbamylation links inflammation, smoking, uremia and atherogenesis, Nat Med 13 (10) (2007) 1176–1184, https://doi.org/10.1038/nm1637.

[38] A. Rajamohan, B. Heit, E. Cairns, L. Barra, Citrullinated and homocitrullinated low-density lipoprotein in rheumatoid arthritis, Scand. J. Rheumatol. 50 (5) (2021) 343–350, https://doi.org/10.1080/03009742.2020.1867237.

[39] R.K. Tangirala, E.M. Rubin, W. Palinski, Quantitation of atherosclerosis in murine models: correlation between lesions in the aortic origin and in the entire aorta, and differences in the extent of lesions between sexes in LDL receptor-deficient and apolipoprotein E-deficient mice, J. Lipid Res. 36 (11) (1995) 2320–2328.

[40] X. Que, M.Y. Hung, C. Yeang, A. Gonen, T.A. Prohaska, X. Sun, et al., Oxidized phospholipids are proinflammatory and proatherogenic in hypercholesterolaemic mice, Nature 558 (7709) (2018) 301–306, https://doi.org/10.1038/s41586-018-0198-8.

[41] A. Gonzalez, H. Maradit Kremers, C.S. Crowson, K.V. Ballman, V.L. Roger, S. J. Jacobsen, et al., Do cardiovascular risk factors confer the same risk for cardiovascular outcomes in rheumatoid arthritis patients as in non-rheumatoid arthritis patients? Ann. Rheum. Dis. 67 (1) (2008) 64–69, https://doi.org/10.1136/ard.2006.059980.

[42] M. McMahon, J. Grossman, J. FitzGerald, E. Dahlin-Lee, D.J. Wallace, B.Y. Thong, et al., Proinflammatory high-density lipoprotein as a biomarker for atherosclerosis in patients with systemic lupus erythematosus and rheumatoid arthritis, Arthritis Rheum. 54 (8) (2006) 2541–2549, https://doi.org/10.1002/art.21976.